

# Clean and Dirty Superconductivity in Pure, Al doped, and Neutron Irradiated $\text{MgB}_2$ : a Far-Infrared Study

M. Ortolani,<sup>1</sup> D. Di Castro,<sup>1,2</sup> P. Postorino,<sup>1</sup> I. Pallecchi,<sup>3</sup> M. Monni,<sup>3</sup> M. Putti,<sup>3</sup> and P. Dore<sup>1</sup>

<sup>1</sup>*Coherentia-INFM and Physics Department,  
University of Rome "La Sapienza",*

*P.le A. Moro 5, I-00185, Rome, Italy*

<sup>2</sup>*Physics Institute, University of Zurich,  
Winterthurerstr. 190, CH-8057, Zurich, Switzerland*

<sup>3</sup>*INFM-LAMIA, Dipartimento di Fisica,  
Via Dodecaneso 33, 16146 Genova, Italy*

## Abstract

The effects of Al substitution and neutron irradiation on the conduction regime (clean or dirty) of the  $\pi$ - and  $\sigma$ -band of  $\text{MgB}_2$  have been investigated by means of far-infrared spectroscopy. The intensity reflected by well characterized polycrystalline samples was measured up to  $100 \text{ cm}^{-1}$  in both normal and superconducting state. The analysis of the superconducting to normal reflectivity ratios shows that only the effect of the opening of the small gap in the dirty  $\pi$ -band can be clearly observed in pure  $\text{MgB}_2$ , consistently with previous results. In Al-doped samples the dirty character of the  $\pi$ -band is increased, while no definitive conclusion on the conduction regime of the  $\sigma$ -band can be drawn. On the contrary, results obtained for the irradiated sample show that the irradiation-induced disorder drives the  $\sigma$ -band in the dirty regime, making the large gap in  $\sigma$ -band observable for the first time in far-infrared measurements.

PACS numbers: 74.70.Ad, 74.25.Gz, 74.62.Dh

A large number of theoretical<sup>1,2</sup> and experimental<sup>3,4,5</sup> works showed that MgB<sub>2</sub> is a two-band superconductor with two distinct energy gaps: a small gap  $\Delta_\pi$  originating from the three-dimensional (3D)  $\pi$ -bands, formed by  $p_z$  orbitals of boron along the  $c$ -axis, and a large gap  $\Delta_\sigma$  originating from the two-dimensional (2D)  $\sigma$ -bands in the  $ab$ -plane, formed by the boron  $sp^2$  hybrids orbitals. Different measurements showed that  $\Delta_\pi$  and  $\Delta_\sigma$  are in the range 1.5-3.5 meV and 6.0-7.5 meV, respectively.<sup>3,4,5</sup> Substitutional impurities introduced in the system can modify the *intraband* impurity scattering in the  $\pi$  and/or  $\sigma$  bands, thus affecting their transport properties. On the contrary, an increase of the small *interband* scattering between  $\pi$  and  $\sigma$  bands is difficult to achieve, owing to the different parity of  $\pi$  and  $\sigma$  orbitals.<sup>6</sup> A large number of studies has then been devoted to investigate the effects of substitutional impurities in MgB<sub>2</sub>, in particular Al for Mg<sup>7,8</sup> and C for B,<sup>9,10,11</sup> which allows to selectively disorder  $\pi$  or  $\sigma$  bands, thus giving the unique opportunity to tune normal and superconducting state properties.

In the case of a conventional (i.e., single-band s-wave) BCS superconductor, characterized by coherence length  $\xi_0$  and energy gap  $\Delta$ , the decrease of the electron mean free-path  $\ell$  due to the increase of impurity scattering modifies the conduction regime, which is classified in the clean-limit when  $\ell > \xi_0$  and in the dirty-limit when  $\ell < \xi_0$ . In studying the conduction regime, infrared spectroscopy can be a powerful tool for investigating important physical quantities such as the gap  $\Delta$ , the plasma frequency  $\Omega$ , and the scattering rate  $\Gamma$ . The optical response of the system is indeed given by the complex optical conductivity  $\sigma(\omega) = \sigma_1(\omega) + i\sigma_2(\omega)$ . In the normal state,  $\sigma_N$  is determined by  $\Omega$  and  $\Gamma$ , accordingly to the standard Drude model. In the superconducting state, accordingly to the Mattis and Bardeen (MB) model, the ratio  $\sigma_S/\sigma_N$  is determined by  $\Delta$ , since, for  $0 < \omega < 2\Delta/\hbar$ ,  $\sigma_{1,S}(\omega) = 0$  and  $\sigma_{2,S}(\omega) \propto 1/\omega$ .<sup>12</sup> Therefore the reflectance spectrum  $R(\omega)$  of a bulk superconductor monotonically increases towards 1 as  $\omega$  goes to 0 in the normal state ( $R_N$ ), while it steeply increases to 1 as  $\omega$  goes to  $2\Delta/\hbar$  in the superconducting state ( $R_S$ ). Therefore, an increase in the  $R_S/R_N$  reflectivity ratio, followed by a maximum around  $\omega = 2\Delta/\hbar$ , is expected on decreasing frequency.<sup>12,13</sup> The same arguments explain the maximum observed in the superconducting to normal transmission ratio obtained on thin superconducting films.<sup>14,15</sup> However, this behavior strongly depends on the conduction regime. In particular, when  $\Gamma \ll 2\Delta/\hbar$ , the maximum disappears since, in the normal state,  $\sigma_{1,S}(\omega)$  is already close to zero at  $\omega = 2\Delta/\hbar$ .<sup>16</sup> It is worth to notice that, in optics, the condition  $\Gamma \ll 2\Delta/\hbar$  ( $\Gamma \gg 2\Delta/\hbar$ ),

which correspond to  $\ell \gg \xi_0$  ( $\ell \ll \xi_0$ ) since  $\ell = v_F/\Gamma$  and  $\xi_0 = \hbar v_F/\pi\Delta$ , is conveniently introduced in defining the clean (dirty) limit condition.<sup>13</sup> In the two-band superconductor  $\text{MgB}_2$ , the situation is far more complex because of the different characteristics of  $\pi$ - and  $\sigma$ -bands. In particular, recent Raman measurements<sup>5</sup> indicate that  $\pi$  and  $\sigma$  carriers are in the dirty and clean regime, respectively. This result is supported by transmittance measurements on  $\text{MgB}_2$  thin films<sup>17,18</sup> and reflectivity measurements on  $\text{MgB}_2$  films<sup>19</sup> and single crystals,<sup>20</sup> where the effect of the small  $\Delta_\pi$  gap (dirty limit) is observed, while no effect of the  $\Delta_\sigma$  gap (clean limit) is revealed.

The aim of the present work was to monitor, by means of far-infrared (FIR) spectroscopy, the effects of disorder induced by Al substitution or neutron irradiation on  $\Gamma$  and  $\Delta$ , i.e. on the conduction regime, of the  $\text{MgB}_2$   $\pi$ - and  $\sigma$ -band. Reflectivity measurements were thus performed in the FIR region on pure  $\text{MgB}_2$  (sample A),  $\text{Mg}_{0.85}\text{Al}_{0.15}\text{B}_2$  (B), and  $\text{Mg}_{0.7}\text{Al}_{0.3}\text{B}_2$  (C) polycrystalline samples. Details on sample preparation and characterization are reported elsewhere.<sup>21</sup> A fourth sample (D), obtained by irradiating  $\text{Mg}^{11}\text{B}_2$  with a thermal neutron fluence of  $10^{18}$  n/cm<sup>2</sup>,<sup>22</sup> was also measured. The values of the parameters which characterize the investigated samples are reported in Table I.  $T_C$  is strongly decreased by Al doping, in agreement with previous reports,<sup>7,8</sup> while it is only slightly reduced by irradiation. The resistivity  $\rho$  at 40 K ( $\rho_{40K}$ ) is as low as  $2.2 \mu\Omega\text{cm}$  for the pure sample, and it increases up to  $24 \mu\Omega\text{cm}$  with Al doping, and to  $20 \mu\Omega\text{cm}$  with irradiation. The energy gaps  $\Delta_\sigma$  and  $\Delta_\pi$  were measured only for the A, B, and C samples by means of point-contact spectroscopy.<sup>21</sup> By using *ab-initio* electronic band-structure computations,<sup>21,23</sup> the doping-dependent anisotropic plasma frequencies ( $\Omega_\sigma^{(a,b)}$ ,  $\Omega_\sigma^{(c)}$ ,  $\Omega_\pi^{(a,b)}$ , and  $\Omega_\pi^{(c)}$ ) were obtained. It is worth to notice that, for pure  $\text{MgB}_2$ , the quoted  $\Omega$  values are well consistent with previous determinations.<sup>1</sup>

Reflectivity measurements were performed in the FIR region up to about  $100 \text{ cm}^{-1}$  with a rapid-scanning Bomem DA3 Michelson interferometer, equipped with a liquid-cooled stabilized Hg lamp, a bolometer cooled at 1.6 K, and different Mylar beamsplitters. Each sample was mounted on the cold head of a cryostat equipped with a temperature controller which allows long-time data acquisition down to 8 K at temperatures stabilized within 0.5 K. The large surface of the samples (around 6 mm in diameter) had an appreciable reflectivity in the visible region although in polycrystalline form. This allowed to carefully align the sample, and to collect the reflected intensity at near-normal incidence using a large dimension IR beam. For each sample, measurements were carried out at 8 K ( $R_S$ ) and at

45 K ( $R_N$ ), in order to directly obtain the  $RR = R_S(8\text{ K})/R_N(45\text{ K})$  reflectivity ratio. This procedure,<sup>24</sup> which does not need reference sample or gold evaporation at room temperature to measure the absolute reflectance, allows to avoid systematic errors due to misalignments of the sample or to additional thermal cycles. Each spectrum was obtained by collecting 5000 interferograms, within an acquisition time of at least 1 hour. The obtained  $RR$  ratios are shown in Figure 1 as a function of the wavenumber  $\nu$ . By considering reproducibility of repeated measurements, the uncertainties on the  $RR$  ratios, mainly due to lamp instability and Fourier transformations, were estimated to be  $\pm 0.005$  and  $\pm 0.002$  at  $30\text{ cm}^{-1}$  and  $70\text{ cm}^{-1}$ , respectively. Low-frequency  $RR$  data on which the uncertainty was larger than 0.005 were discarded.

A first inspection of Fig. 1 shows that for the pure  $\text{MgB}_2$  sample (panel a) the  $RR$  ratio clearly increases below the frequency-edge around  $50\text{ cm}^{-1}$  ( $\simeq 6\text{ meV}$ ), in agreement with a previous FIR study on polycrystalline  $\text{MgB}_2$ .<sup>24</sup> As discussed above, this increase can be attributed to the optical effect of the  $\Delta_\pi$  gap, while no clear effect of the  $\Delta_\sigma$  gap is observable. In the Al doped samples (panels b, c),  $RR$  does not drastically change with respect to the pure  $\text{MgB}_2$  case. However, the small edge shift, observed on going from  $x=0.0$  to  $x=0.3$ , is not consistent with the strong decrease of  $\Delta_\pi$  (see Table I). This suggests that the effect of the  $\Delta_\sigma$  gap, although not directly detectable, is not negligible in the Al-doped samples. In the case of the irradiated sample (panel d), on the contrary, remarkable changes in both shape and intensity are observed. In particular,  $RR$  starts to increase around  $90\text{ cm}^{-1}$ . We remark that this behavior cannot be explained by an optical effect of the  $\Delta_\pi$  gap, but must be ascribed to an optical signature of the  $\Delta_\sigma$  gap.

To determine  $\Gamma$  and  $\Delta$  from the measured  $RR$  reflectivity ratios, it is necessary to model the complex optical conductivity  $\sigma$  in both normal ( $\sigma_N$ ) and superconducting ( $\sigma_S$ ) states. In the normal state,  $\sigma_N(\Omega, \Gamma; \omega)$  is provided by the Drude model, which is well reliable below  $100\text{ cm}^{-1}$  since in this low energy range neither optical phonon absorption or frequency dependence of  $\Gamma$  occur. In the superconducting state the model developed by Zimmermann et al.<sup>26</sup> was employed, as in previous analysis of  $\text{MgB}_2$  FIR spectra.<sup>18,19</sup> This model generalizes the MB theory and provides  $\sigma_S(\Omega^2/\Gamma, \Gamma, \Delta, T; \omega)$  at any given temperature  $T < T_c$  for an arbitrary scattering rate  $\Gamma$ . For a conventional superconductor, test calculations showed that the maximum in the resulting  $R_S/R_N$  is evident when the ratio  $\Gamma/(2\Delta/\hbar)$  is at least of the order of 2. In the  $\text{MgB}_2$  case it is necessary to consider both  $\pi$ - and  $\sigma$ -band contribu-

tions to the  $ab$ -plane ( $\sigma^{(ab)}$ ) and  $c$ -axis ( $\sigma^{(c)}$ ) conductivities. For example, the normal state conductivities are given by:

$$\sigma_N^{(x)}(\omega) = \frac{[\Omega_\sigma^{(x)}]^2/\Gamma_\sigma}{1 + i\omega/\Gamma_\sigma} + \frac{[\Omega_\pi^{(x)}]^2/\Gamma_\pi}{1 + i\omega/\Gamma_\pi} \quad (1)$$

with  $(x)=(a,b)$  or  $(c)$ . Since each  $\sigma^{(x)}$  gives the reflectivity  $R^{(x)}$ , the reflectivity  $R$  of the polycrystalline sample can finally be evaluated as  $R=(1/3)R^{(c)} + (2/3)R^{(a,b)}$ ,<sup>25</sup> since it is reasonable to assume that a large number of randomly oriented crystallites are impinged by the wide IR beam.

The model  $R_S/R_N$  curve was fitted to the experimental  $RR$  by employing only  $\Delta_\pi, \Delta_\sigma, \Gamma_\pi$ , and  $\Gamma_\sigma$  as free parameters, since the plasma frequencies  $\Omega$  cannot be obtained by the present reflectivity measurements carried out over a very limited spectral range. It is well known that in  $\text{MgB}_2$  a strong discrepancy exists between the  $\Omega$  calculated<sup>1</sup> and those observed in reflectance measurements,<sup>17,18,20,25</sup> being the latter typically smaller by a factor five than the former. A discussion of this discrepancy, which is not yet fully understood,<sup>25</sup> is beyond the aim of the present paper. The computed  $\Omega$  values (see Table I) divided by a factor 5 were thus employed. For the irradiated sample D, the pure  $\text{MgB}_2$   $\Omega$  values were used, by assuming that irradiation does not appreciably affect the electronic band structure, as can be evinced by the weak reduction of  $T_C$  in sample D (Table I).

Figure 1 shows that a satisfactory agreement is obtained between the experimental data and the best-fit curves for pure and Al-doped samples (panels a, b, and c). The best-fit values of  $\Gamma$  and  $\Delta$  are reported in Table I. The quoted errors on the parameter values represent the range over which the parameters can be varied without appreciably affecting the quality of the fit. Note that in Al-doped samples the  $RR$  curves were fitted up to a maximum frequency corresponding to three times the  $\Delta_\sigma$  values provided by point-contact measurements (see Table I). Approximations involved in the employed procedure indeed are not expected to provide a reliable estimate of  $R_S/R_N$  at higher frequencies.<sup>27</sup> Also note that in Table I and in the following of the paper the  $\Gamma$  and  $\Delta$  values are given in meV units, for easier comparison with previously reported values. For pure  $\text{MgB}_2$ , the  $\Delta_\pi$  and  $\Gamma_\pi$  values are determined with good accuracy since the fit is very sensitive to the conduction regime of the dirty  $\pi$ -band, which basically determines the edge position of the  $R_S/R_N$  increase. The  $\Delta_\sigma$  and  $\Gamma_\sigma$  values for this sample are not reported since these quantities cannot be unambiguously determined for a band in the clean limit.<sup>16</sup> Indeed, varying the values of  $(\Delta_\sigma, \Gamma_\sigma)$  within the range (5

meV, 2 meV) $\div$ (12 meV, 10 meV) has no effect on the fit results for  $\Delta_\pi$  and  $\Gamma_\pi$ . In the case of the  $\text{Mg}_{1-x}\text{Al}_x\text{B}_2$  samples,  $\Delta_\pi$  and  $\Gamma_\pi$  are obtained with good accuracy, as in pure  $\text{MgB}_2$ . Although with large uncertainties, also  $\Delta_\sigma$  and  $\Gamma_\sigma$  are determined, which indicates that the effect of the  $\Delta_\sigma$  gap is not negligible in the Al doped samples. It is remarkable that the  $\Delta_\pi$  values determined in this work are very close to those directly measured with point-contact spectroscopy (see Table I),<sup>21</sup> and to those determined through specific-heat measurements.<sup>28</sup> In addition the present work provides a valuable determination of the Al-doping dependence of  $\Gamma_\pi$ , which increases by a factor 3 when the Al-doping is increased up to 30%.

For the neutron irradiated sample, Fig. 1d shows that a good agreement is obtained between experimental  $RR$  and computed  $R_S/R_N$ . A small uncertainty affects all the best-fit parameter values (see Table I) since in this case both the  $\pi$  and  $\sigma$  bands play an important role in determining shape and absolute values of  $R_S/R_N$ . It is worth to notice that the  $\Delta_\pi$  and  $\Delta_\sigma$  values (not directly measured in the irradiated sample) are very close to those of pure  $\text{MgB}_2$ . This result was expected since the  $T_C$  of the irradiated sample is close to that of pure  $\text{MgB}_2$ . On the other hand, the relaxation rates  $\Gamma$  are strongly increased with respect to the pure sample and, noticeably, they are nearly the same in  $\pi$  and  $\sigma$  bands, showing that the disorder introduced by irradiation is not preferentially located in Mg or B planes.

Since the present analysis does provide a self-consistent estimate of the effect of Al-doping or irradiation on the  $\Gamma$  and  $\Delta$  values, we finally report in Table I the resulting  $\Gamma_\pi/2\Delta_\pi$  and  $\Gamma_\sigma/2\Delta_\sigma$  ratios, which characterize the conduction regime of the  $\pi$ - and  $\sigma$ -bands. As for the  $\pi$ -band, the  $\Gamma_\pi/2\Delta_\pi$  values confirm the dirty character of this band, which is increased by Al-doping (samples B and C). It is worth to notice that the  $\Gamma_\pi/2\Delta_\pi$  value in sample D is much higher than in pure  $\text{MgB}_2$ , owing mainly due to the high  $\Gamma_\pi$  value induced by irradiation. As for the  $\sigma$ -band, no definitive assessment can be made on its conduction regime for Al doped samples, owing to the large errors affecting  $\Gamma_\sigma/2\Delta_\sigma$  (see Table I). However, the present results suggest that, with increasing Al doping, the  $\sigma$ -band also moves towards a dirty regime, due to the combined effect of the large decrease of  $\Delta_\sigma$  and the small increase of  $\Gamma_\sigma$ . This is consistent with a previous study of the Al-doping dependence of the upper critical field  $B_{C2}$  indicating the dirty character of the  $\sigma$ -band in the  $x=0.3$  sample.<sup>21</sup> In the irradiated sample  $\Gamma_\sigma/2\Delta_\sigma > 2$ , owing mainly to the strong increase of  $\Gamma_\sigma$ . This, combined with the high value of  $\Delta_\sigma$ , makes well apparent the effect of the  $\sigma$ -gap. We remark that this result allows to clearly assess the dirty character of the  $\sigma$ -band in the irradiated sample, in

agreement with the upper critical field analysis.<sup>22</sup>

In considering the results obtained for the  $\sigma$  band in Al-doped samples, it is worth to notice that the effect of the  $\sigma$ -band on  $R_S/R_N$  could be much more clearly tested by probing the optical response of only the  $ab$ -plane, thus avoiding the  $c$ -axis contribution which is dominated by carriers in the dirty  $\pi$ -band. FIR measurements on the  $ab$  face of aluminum- and carbon-substituted single crystals<sup>11</sup> are thus in program.

In conclusion, the dirty character of the  $\pi$ -band in all the investigated  $\text{MgB}_2$  samples is clearly evidenced by present results. In Al-doped samples, no definitive assessment can be made on the conduction regime of the  $\sigma$ -band, although obtained results suggest that it moves towards a dirty regime with increasing Al doping. On the contrary, results obtained for the irradiated sample show that the irradiation-induced disorder in both the Mg and B planes drives the  $\sigma$ -band in the dirty regime without significantly reducing  $T_C$  and  $\Delta_\sigma$ , thus making the  $\text{MgB}_2$   $\sigma$ -gap observable for the first time in FIR measurements. Irradiation therefore can provide an efficient method for obtaining a dirty  $\text{MgB}_2$  superconductor with high  $T_C$ .

The authors thank P. Manfrinetti and A. Palenzona who prepared the samples studied in this work.

---

<sup>1</sup> A.Y. Liu, I.I. Mazin, and J. Kortus, Phys. Rev. Lett. **87**, 087005 (2001).

<sup>2</sup> H.J. Choi, D. Roundy, H. Sun, M.L. Cohen, and S.G. Louie, Phys. Rev. B **66**, 020513 (2002).

<sup>3</sup> F. Bouquet, Y. Wang, R.A. Fisher, D.G. Hinks, J.D. Jorgensen, A. Junod, and N.E. Phillips, Europhys. Lett. **56**, 856 (2001)

<sup>4</sup> R.S. Gonnelli, D. Daghero, G.A. Ummarino, V.A. Stepanov, J. Jun, S.M. Kazakov, and J. Karpinski, Phys. Rev. Lett. **89**, 247004 (2002)

<sup>5</sup> J.W. Quilty, S. Lee, S. Tajima, and A. Yamanaka, Phys. Rev. Lett. **90**, 207006 (2003).

<sup>6</sup> I.I. Mazin, O.K. Andersen, O. Jepsen, O.V. Dolgov, J. Kortus, A.A. Golubov, A.B. Kuz'menko,, and D. van der Marel, Phys. Rev. Lett. **89**, 107002 (2002)

<sup>7</sup> J.S. Slusky, N. Rogado, K.A. Regan, M.A. Hayward, P. Kalifah, T. He, K. Inumaru, S.M. Loureiro, M.K. Haas, H.W. Zanderbergen, and R.J. Cava R.J., Nature **410**, 343 (2001)

<sup>8</sup> A. Bianconi, S. Agrestini, D. Di Castro, G. Campi, G. Zangari, N. L. Saini, A. Saccone, S. De



- Negri, M. Giovannini, G. Profeta, A. Continenza, G. Satta, S. Massidda, A. Cassetta, A. Pifferi, and M. Colapietro, Phys. Rev. B **65**, 174515 (2002)
- <sup>9</sup> T. Masui, S. Lee, and S. Tajima, Phys. Rev. B **70**, 024504 (2004)
- <sup>10</sup> R.H.T.Wilke, S.L.Bud'ko, P.C.Canfield, D.K.Finnemore, R.J.Suplinskas, S.T.Hannahs, Phys. Rev. Lett. **92**, 217003 (2004)
- <sup>11</sup> S.M. Kazakov, R. Puzniak, K. Rogacki, A.V. Mironov, N.D. Zhigadlo, J. Jun, Ch. Soltmann, B. Batlogg, and J. Karpinski, cond-mat/0405060.
- <sup>12</sup> M. Tinkham, *Introduction to Superconductivity*, McGraw-Hill, New York (1975).
- <sup>13</sup> T. Timusk and D. Tanner, in Physical Properties of High Temperature superconductors, ed. D.M. Ginsberg, World Scientific, Singapore (1989).
- <sup>14</sup> D.M. Ginsberg and M. Tinkham, Phys. Rev. **118**, 990 (1960).
- <sup>15</sup> G.P. Williams, R.C. Budhani, C.J. Hirschmugl, G.L. Carr, S. Perkowitz, B. Lou, and T.R. Yang, Phys. Rev. B **41**, 4752 (1990).
- <sup>16</sup> K.Kamaras, S.L.Herr, C.D.Porter, N.Tache, D.B.Tanner, S.Etemad, T.Venkatesan, E.Chase, A.Inam, X.D.Wu, M.S.Hedge, B.Dutta, Phys.Rev.Lett. **64**, 84 (1990).
- <sup>17</sup> R.A. Kaindl, M.A. Carnahan, J. Orenstein, D.S. Chemla, H.M. Christen, H.Y. Zhai, M. Paranthaman, and D.H. Lowndes, Phys. Rev. Lett. **88**,027003 (2002).
- <sup>18</sup> J.H. Jung, K.W. Kim, H.J. Lee, M.W. Kim, T.W. Noh, W.N. Kang, H.J. Kim, E.M. Choi, C.U. Jung, and S.I. Lee, Phys. Rev. B **65**, 052413 (2002).
- <sup>19</sup> A. Pimenov, A. Loidl, and S.I. Krasnosvobodtsev, Phys. Rev. B **65**, 172502 (2002)
- <sup>20</sup> A. Perucchi, L. Degiorgi, J. Jun, M. Angst, and J. Karpinski, Phys. Rev. Lett. **89**, 097001 (2002)
- <sup>21</sup> M. Putti, C. Ferdeghini, M. Monni, I. Pallecchi, C. Tarantini, P. Manfrinetti, A. Palenzona, D. Daghero, R.S. Gonnelli, and V.A. Stepanov, cond-mat/0406377
- <sup>22</sup> M.Putti, V.Braccini, C.Ferdeghini, I.Pallecchi, A.S.Siri, F.Gatti, P.Manfrinetti, A.Palenzona, Phys.Rev.B **70**, 052509 (2004)
- <sup>23</sup> G. Profeta, A. Continenza, and S. Massidda, Phys. Rev. B **68**, 144508 (2003).
- <sup>24</sup> B. Gorshunov, C.A. Kuntscher, P. Haas, M. Dressel, F.P. Mena, A.B. Kuz'menko, D. van der Marel, T. Muranaka, and J. Akimitsu, Eur. Phys. J. B **21**, 159 (2001)
- <sup>25</sup> Y. Fudamoto and S. Lee, Phys. Rev. B **68**, 184514 (2003).
- <sup>26</sup> W. Zimmermann, E.H. Brandt, M. Bauer, E. Seider, and L. Genzel, Physica C **183**, 99 (1991).



- <sup>27</sup> H.S. Somal, B.J. Feenstra, J. Schutzmann, J.H. Kim, Z.H. Barber, V.H.M. Duijn, N.T. Hien, A.A. Menovsky, M. Palumbo, and D. van der Marel, Phys. Rev. Lett. **76**, 1525 (1996).
- <sup>28</sup> M. Putti, M. Affronte, P. Manfrinetti, and A. Palenzona, Phys. Rev. B **68**, 094514 (2003).

TABLE I: Parameters characterizing the investigated  $\text{MgB}_2$  (A),  $\text{Mg}_{0.85}\text{Al}_{0.15}\text{B}_2$  (B),  $\text{Mg}_{0.7}\text{Al}_{0.3}\text{B}_2$  (C), and neutron irradiated  $\text{MgB}_2$  (D) samples. Uncertainties on the last digit are reported in brackets.  $\ddagger$  indicates parameter values from Refs. 21,22,  $\dagger$  calculated plasma frequencies, and FIR parameter values obtained from the fitting procedure (see text).

		A	B	C	D
$\ddagger$	$T_C(\text{K})$	39.0(2)	31(2)	24(3)	36.3(2)
	$\rho_{40K}(\mu\Omega\text{cm})$	2.2(2)	12(1)	24(2)	20(2)
	$\Delta_\sigma(\text{meV})$	7.4(5)	4(1)	2.0(2)	—
	$\Delta_\pi(\text{meV})$	2.8(1)	1.7(2)	0.5(2)	—
$\dagger$	$\Omega_\sigma^{(a,b)}(\text{eV})$	3.8	3.2	2.6	—
	$\Omega_\sigma^{(c)}$	0.7	0.7	0.7	—
	$\Omega_\pi^{(a,b)}$	5.5	5.9	6.0	—
	$\Omega_\pi^{(c)}$	6.4	6.8	6.9	—
FIR	$\Delta_\sigma(\text{meV})$	—	3.0(8)	3(1)	6.6(6)
	$\Gamma_\sigma$	—	9(3)	11(4)	31(4)
	$\Delta_\pi$	2.4(2)	1.7(4)	1.2(3)	2.2(2)
	$\Gamma_\pi$	11(1)	19(2)	27(3)	31(3)
	$\Gamma_\sigma/2\Delta_\sigma$	—	1.6(5)	2.0(7)	2.4(3)
	$\Gamma_\pi/2\Delta_\pi$	2.4(3)	5.4(8)	11(2)	7.0(8)

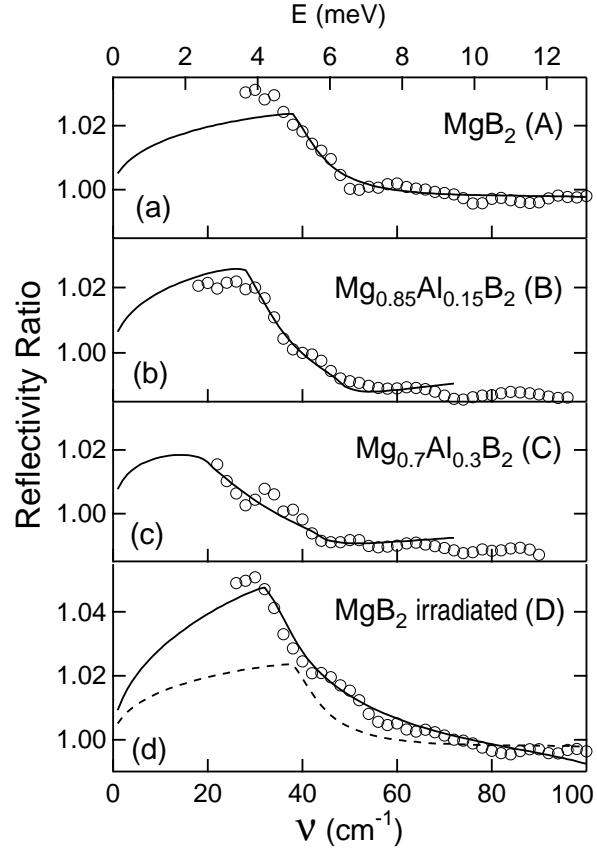


FIG. 1: Measured  $RR$  (open symbols) and best-fit  $R_S/R_N$  (full lines) reflectivity ratios. In panel (d) the best-fit  $R_S/R_N$  of pure  $\text{MgB}_2$  (panel a) is reported for comparison (dashed line).